

Fabrication and Laser Behavior of Composite Yb:YAG Ceramic

Fei Tang,^{§,¶} Yongge Cao,^{§,||,‡,†} Jiquan Huang,[§] Huagang Liu,[§] Wang Guo,[§] and Wenchao Wang^{||}

[§]Key Lab of Optoelectronic Materials Chemistry and Physics, Fujian Institute of Research on the Structure of Matter, Chinese Academy of Sciences, Fuzhou 350002, China

[¶]Graduate School of the Chinese Academy of Sciences, Beijing 100039, China

^{||}Department of Physics, Renmin University of China, Beijing 100872, China

Fifteen layers' composite YAG/Yb:YAG/YAG laser ceramic with grain size of about 5 μm was fabricated through tape casting process together with vacuum sintering technology, and its microstructure, optical properties, and laser performance were investigated. The experimental results showed that annealing in oxygen atmosphere could remove the lattice distortion and improve the optical transmittance. The in-line transmittance was 83% at 800 nm. The laser study indicated that the threshold pump power was 5.5 W with output coupler transmission of 6% and slope efficiency achieved 12%. The maximum output power of 0.53 W was achieved at the absorbed pump power of 10 W.

I. Introduction

OPTICAL grade ceramics have been widely considered as promising substitute for mono-crystal and the next generation of laser gain media,¹ due to their remarkable advantages, such as high doping concentration, low cost,² high-dopant homogeneity, easy fabrication of large size sample, and realizability of multilayer structure.³ Among all these advantages, the realizability of multilayer structure is very attractive, because it means the realizability of multifunction and optimization of properties. For example, more effective thermal management during laser operation process can be achieved by adjusting the doping concentration of rare earth ions into the host materials (i.e., by the fabrication of multilayer structure with different doping concentrations) because the exponential decay of the pump light distribution can be overcome, and thereby the longitudinal temperature and mechanical stress gradient in end-pumped solid-state lasers can be minimized.⁴

However, the fabrication of multilayer composite laser ceramics is very difficult. In general, it requires complicated equipments and fabrication process. Although continuous wavelength (C. W.) laser operation in Nd-doped yttrium aluminum garnet (Nd:YAG) and Yb-doped Y_2O_3 or YAG (Yb: Y_2O_3 or Yb:YAG) have been demonstrated,^{1,2,5–7} there are still few reports on the fabrication of high quality multilayer

laser ceramics. In 2009, Lee *et al.* fabricated multilayer Nd:YAG composite ceramic by tape casting and hot-isostatic press (HIP) technology.⁸ However, laser output was not achieved. In 2010, Ter-Gabrielyan *et al.* reported the composite ceramic Er:YAG laser by the similar technology which can be described as follows: first, green ceramic was fabricated by tape casting. Then, the sample was vacuum-sintered at a high temperature. Finally, the sample was further sintered under HIP conditions.⁹ It seems that tape casting process has great potential in fabricating multilayer composite laser ceramics through these studies.

In this research, 15 layers' composite Yb:YAG laser ceramic with high doping concentration of 20 at.% was successfully fabricated by tape-casting-assisted vacuum sintering technology. The C. W. laser operation was realized at 1030 nm using as-obtained ceramic as laser gain media. To the best of our knowledge, this is the first report on the fabrication of multilayer composite laser ceramic by simple vacuum sintering technology. Besides, the 20 at.% Yb doping concentration is also the highest doping concentration of Yb:YAG ceramic to achieve laser oscillation.

II. Experiment Procedure

(1) Material Fabrication

Transparent Yb:YAG composite ceramics were fabricated by the tape casting and vacuum sintering approach. The source powders were high-purity Y_2O_3 (99.99%; Alfa Aesar, Ward Hill, MA) with mean size of about 5 μm , $\alpha\text{-Al}_2\text{O}_3$ (99.99%; Sumitomo Chemical Co. Ltd, Osaka, Japan) with mean size of about 200nm, and Yb_2O_3 (99.99%; Alfa Aesar) with mean size of about 3 μm (Fig. S1). In accordance with stoichiometric YAG and 20 at.% Yb:YAG, they were weighted. Then, they at first were milled in solvent for 24 h with 5 wt% fish oil as dispersant. The used solvent is the mixture of ethanol and xylene with weight ratio of 1:1. The solvent and powder weigh ratio is 7:13. Followed by addition of plasticizers (3 wt% Polyalkylene Glycol [PAG] and 3 wt% Butyl Benzyl Phthalate [BBP]) and binder (6 wt% Polyvinyl Butyral [PVB]), the slurries were milled for another 24 h. The obtained slurries were de-aired in vacuum condition and then, cast to form thin tapes with single layer thickness of 0.15 mm. The tapes were cut into pieces that were stacked and laminated (i.e., bonded using heat at the temperature of 120°C and under pressure of 18 MPa) into green parts. The organic content of the parts was burned off in oxygen atmosphere prior to vacuum sintering at 1730°C for 20 h. During the densification, the powders form YAG and 20 at.% Yb:YAG *in situ* as the oxide source powders react. A few, about 2.2-mm-thickness three-segment composite disks with segments of undoped YAG, 20 at.% Yb:YAG, and undoped YAG were fabricated, as shown in Fig. 1. The annealing treatment was car-

V. B. Kravchenko—contributing editor

Manuscript No. 30273. Received September 05, 2011; approved October 22, 2011.

This work was financially supported by the Key Program in Major Research Plan of National Natural Science Foundation of China (91022035), Main Direction Program of Knowledge Innovation of Chinese Academy of Sciences, "Hundred Talents Program" of the Chinese Academy of Sciences, and National High-tech R&D Program of China (863 Program).

[¶]Present address: 155 Yangqiao West Road Fuzhou 350002 China.

[†]Author to whom correspondence should be addressed. e-mail: caoyongge@fjirsm.ac.cn.

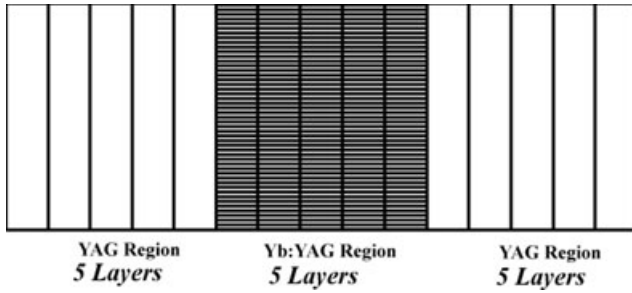


Fig. 1. Design scheme of composite Yb:YAG ceramics.

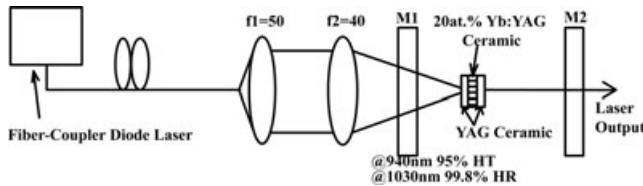


Fig. 2. Scheme of laser system: M1, input mirror; M2, output coupler mirror.

ried out under oxygen atmosphere at 1450°C for 10 h. Both surfaces were mirror-polished for optical measurement.

(2) Laser Measurement

The laser cavity of an end-pumped plano-plano resonator with total cavity length of about 35mm is used, as shown in Fig. 2. Composite ceramic with size of 10 mm \times 10 mm \times 2 mm is pumped by 940 nm fiber couple LD pumping source with a core diameter of 400 μ m. Two convex lenses, having focal length of 50 and 40 mm, respectively, are used to focus the pump beam into the ceramic specimen and the pump light footprint is about 300 μ m. The total cavity is mainly composed of two mirrors, the input mirror and output coupler. The former has 95% transmission at 940 nm and 99.8% reflectivity at 1030 nm. Output coupler with transmission of 2.3% was used to measure laser performance. The composite ceramic is placed as close as possible to the input mirror and held on the brass mount. Cooling system of cycle water is adopted and the temperature is set about 20°C.

III. Results and Discussion

Figure 3 shows the SEM images of the YAG/Yb:YAG/YAG composite ceramics. Obviously, the sample was pore-free and there was no evidence of abnormal grain growth. The average grain size was about 5 μ m. Full dense microstructure without obvious trace of interfaces between adjacent layers was further demonstrated in the cross-section image [Fig. 3(b)]. The simultaneous elimination of pores and interfaces was of significant importance for the improvement of optical transmittance.

Figure 4 shows the photos of this three-segment (15 layers) composite ceramics. For the unannealed sample, as shown in Fig. 4(a), the color of the 20 at.% Yb:YAG segment (i.e., the central part) was dark green, which can be attributed to the formation of oxygen vacancies and Yb^{2+} ions during vacuum sintering. The multilayer composite ceramic was sintered under vacuum and high-temperature condition. Doubtlessly, a lot of oxygen vacancies were generated and part of Yb^{3+} ions were reduced to Yb^{2+} . Consequently, Re-F color centers were introduced, leading to the generation of color.¹⁰ Correspondingly, two broad adsorption peaks were observed in the visible region (centered at about 380 and 640 nm, respectively) in the in-line transmittance spectrum, as shown in Fig. 5. By annealing in oxygen atmosphere at a high temperature for a long time, almost all of the

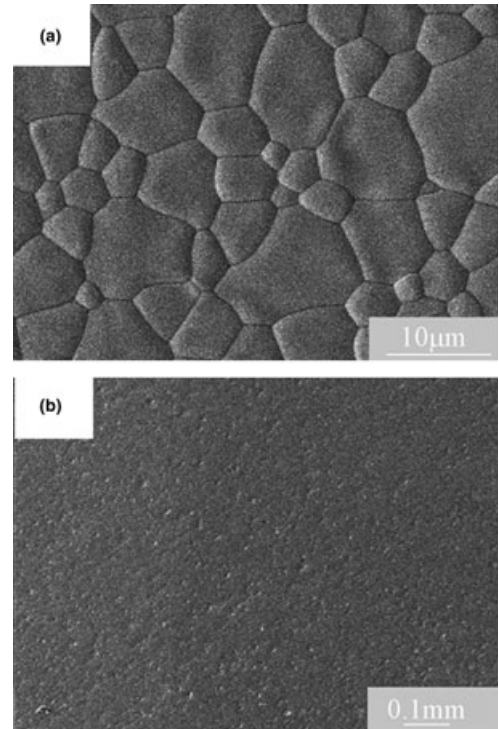


Fig. 3. SEM images of the studied composite ceramic on: (a) Surface morphology; (b) Cross-section morphology.

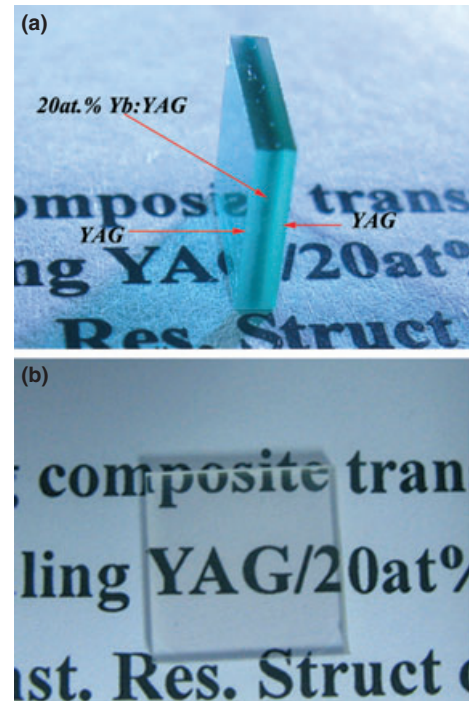


Fig. 4. Photos of composite Yb:YAG ceramic: (a) Before annealing; (b) Postannealing.

oxygen vacancies were eliminated, and most of the Yb^{2+} ions were converted to Yb^{3+} , resulting in the disappearance of the two adsorption peaks in the visible region (Fig. 5), and consequently, the transformation of the color from green to colorless [Fig. 4(b)].

Figure 4 also suggests that both the annealed and unannealed samples were highly transparent, which was further demonstrated by the in-line transmittance spectrum, as shown in Fig. 5. For example, for the annealed sample, about 83% of optical transmittance at 800 nm was achieved.

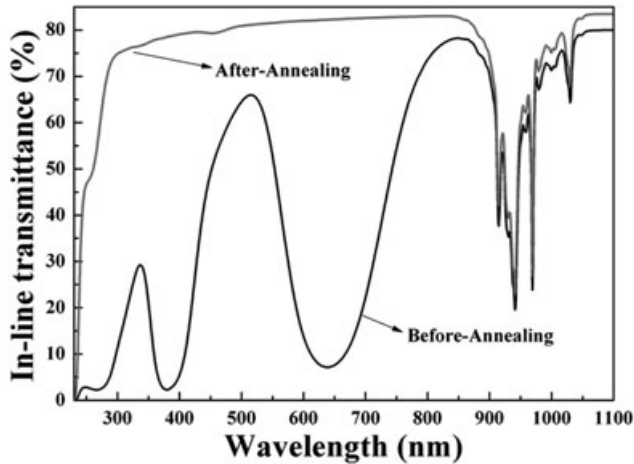


Fig. 5. In-line transmittance spectra for ceramics before and after annealing.

It was further found that the annealed sample showed higher optical transmittance than the unannealed one. The improvement of the transmittance by annealing treatment was attributed to the elimination of lattice stress and vacancies.¹¹ As discussed above, both oxygen vacancies and Yb^{2+} were generated during the high-temperature vacuum sintering. The radius of Yb^{2+} ($R_{\text{Yb}^{2+}} = 1.13 \text{ \AA}$ while $R_{\text{Yb}^{3+}} = 0.99 \text{ \AA}$) is larger than that of Y^{3+} ($R_{\text{Y}^{3+}} = 1.02 \text{ \AA}$). Both the formation of oxygen vacancies and the occupancy of Yb^{2+} in Y^{3+} site in the octahedral structure could lead to the lattice distortion, and consequently, enhanced the lattice stress.

Figure 6 displays the room-temperature normalized absorption and emission spectra of the annealed composite ceramic. This sample had strong electron transition behavior, and this was most prominent in the absorption feature. Three strong absorption peaks, located at 915, 941, and 969 nm, with full width at half maximum (FWHM) of 8, 19, and 4 nm, respectively, were observed. Among them, either the 941 or the 969 nm could be taken as pumping wavelength. From the emission spectrum, it was found that the laser transition at 1030 nm (terminating at 613 cm^{-1} in the ground-state manifold) was the strongest emission feature, and the emission cross-section was calculated to be $2.0 \times 10^{-20} \text{ cm}^2$ at 1030 nm, which is close to that of Yb:YAG single crystal.¹² This wavelength was usually considered as laser wavelength. However, a small absorption peak at 1030 nm was also observed in the absorption spectrum, which indicated the possibility of the some unavoidable impurities (e.g., Er^{3+} , Tm^{3+} , and Ho^{3+}), as well as Yb^{3+} ions self-absorption effect. In general, these two factors probably generate thermal lens effect, which would strengthen

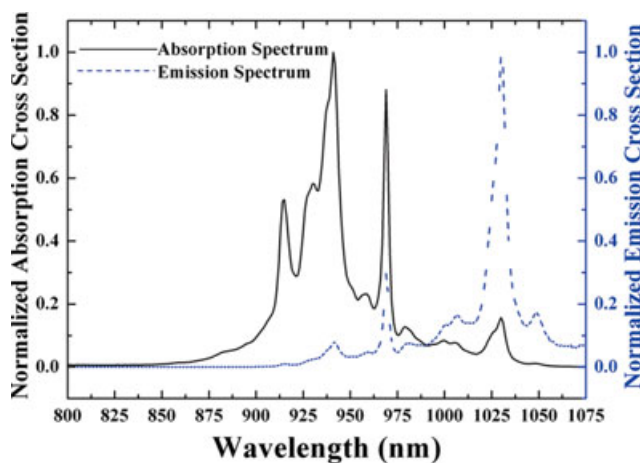


Fig. 6. Absorption and emission spectra for the annealed ceramic.

with increasing pumping power and/or operating time during laser experiment, and therefore, depress the efficient laser output at 1030 nm, and even lead to laser wavelength deviation or laser quenching. The design of Yb:YAG composite structure with different doping concentration of Yb ions was thought to be one of the effective route to overcome thermal lens effect and to stabilize the laser output at 1030 nm.⁴ Figure 7 shows the fitted fluorescence decay curve of composite ceramic, and the lifetime at 1030 nm can be obtained to be 1.76 ms. This value is higher than that in the literature,¹² which further implies the little influence of quenching centers, for example, trace impurities, on fluorescence properties.

Figure 8 shows the laser output power versus the absorbed pump power for the annealed composite ceramic with output coupler transmission of 6%. The C.W. laser output was realized when the pump power was higher than the threshold value of 5.5 W, and the slope efficiency was 12%. The maximum output power was 0.53 W at the pump power of 10 W, corresponding to the optical to optical conversion efficiency of 5.3%. This is the first report on the realization of laser output for multilayer Yb:YAG composite ceramic fabricated by simple vacuum sintering technology.

IV. Summary

Fifteen layers' composite YAG/Yb:YAG/YAG laser ceramic with average grain size of about $5 \mu\text{m}$ was successfully fabricated by tape casting and simple vacuum sintering. Oxygen

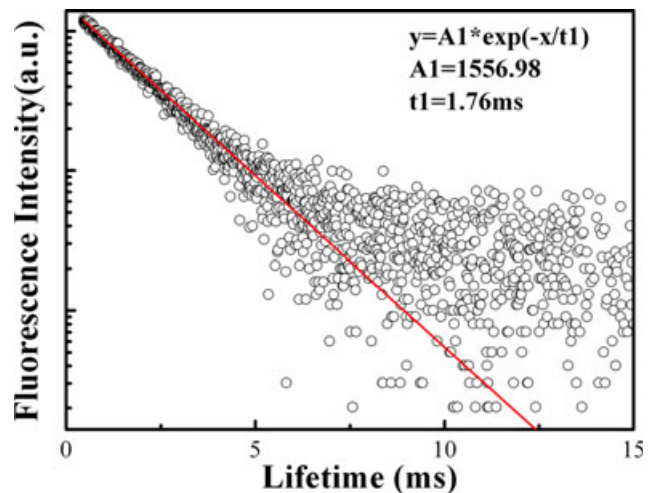


Fig. 7. Fluorescence decay curve of composite YAG/20 at.% Yb:YAG/YAG ceramic.

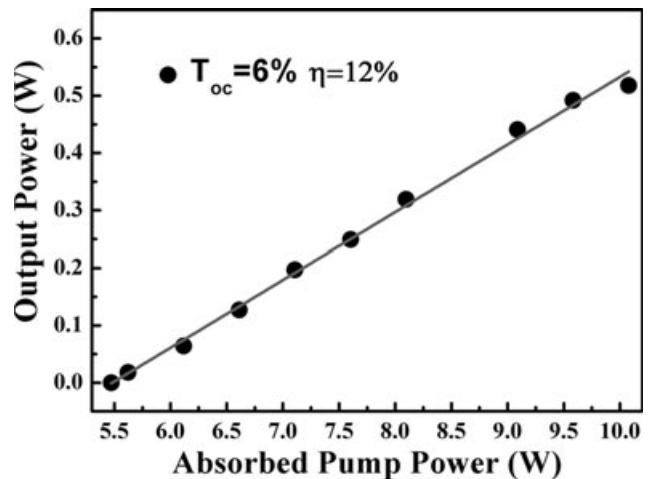


Fig. 8. Laser output power as a function of absorbed pump power.

vacancies were eliminated and Yb^{2+} ions were converted to Yb^{3+} by annealing the ceramic in oxygen atmosphere. The in-line transmittance was 83% at 800 nm. The laser performance was investigated using 940 nm as pumping source and C. W. laser output was generated at 1030 nm. The threshold pump power was 5.5 W and the slope efficiency attained to be 12%. The maximum output power of 0.53 W was achieved at the pump power of 10 W with the optical conversion efficiency of about 5.3%. The results of laser experiment show that this composite ceramic can be used as a laser gain medium. We believe that higher laser output will be realized soon by the modification of precursor powders and improvement of fabrication details in the further study.

Supporting Information

Additional Supporting Information may be found in the online version of this article:

Fig. S1. SEM images of the precursor powders: (a) Al_2O_3 , (b) Y_2O_3 , (c) Yb_2O_3 , and (d) mixed powders after first milled.

Please note: Wiley-Blackwell are not responsible for the content or functionality of any supporting materials supplied by the authors. Any queries (other than missing material) should be directed to the corresponding author for the article.

References

¹D. Kracht, M. Frede, R. Wilhelm, and C. Fallnich, "Comparison of Crystalline and Ceramic Composite Nd:YAG for High Power Diode End-Pumping," *Opt. Express*, **13** [16] 6212–6 (2005).

²A. Ikesue, T. Kinoshita, K. Kamata, and K. Yoshida, "Fabrication and Optical Properties of High-Performance Polycrystalline Nd:YAG Ceramics for Solid-State Lasers," *J. Am. Ceram. Soc.*, **78** [4] 1033–40 (1995).

³J. Lu, M. Prabh, J. Song, C. Li, J. Xu, K. Ueda, A. A. Kaminskii, H. Yagi, and T. Yanagitani, "Optical Properties and Highly Efficient Laser Oscillation of Nd:YAG Ceramics," *Appl. Phys. B*, **71** [4] 469–73 (2000).

⁴D. Kracht, R. Wilhelm, and M. Frede, "407 W End-Pumped Multi-Segmented Nd:YAG Laser," *Opt. Express*, **13** [25] 10140–4 (2005).

⁵J. Kong, D. Y. Tang, B. Zhao, J. Lu, K. Ueda, H. Yagi, and T. Yanagitani, "9.2-W Diode-End-Pumped $\text{Yb}:\text{Y}_2\text{O}_3$ Ceramic Laser," *Appl. Phys. Lett.*, **86** [16] 161116, 3pp (2005).

⁶J. Dong, A. Shirakawa, K. Ueda, H. Yagi, T. Yanagitani, and A. A. Kaminskii, "Efficient $\text{Yb}^{3+}:\text{Y}_3\text{Al}_5\text{O}_{12}$ Ceramic Microchip Lasers," *Appl. Phys. Lett.*, **89** [9] 091114, 3pp (2006).

⁷Q. Liu, M. Gong, W. P. Gong, C. Li, and D. D. Ma, "Corner-Pumped Yb:Yttrium Aluminum Garnet Slab Laser Emitted up to 1 kW," *Appl. Phys. Lett.*, **88** [10] 101113, 3pp (2009).

⁸S. H. Lee, E. R. Kupp, A. J. Stevenson, J. M. Anderson, G. L. Messing, X. Li, E. C. Dickey, J. Q. Dumm, V. K. Simonaitis-Castillo, and G. J. Quarles, "Hot Isostatic Pressing of Transparent Nd:YAG Ceramics," *J. Am. Ceram. Soc.*, **92** [7] 1456–63 (2009).

⁹N. Ter-Gabrielyan, L. D. Merkle, E. R. Kupp, G. L. Messing, and M. Dubinskii, "Efficient Resonantly Pumped Tape Cast Composite Ceramic Er:YAG Laser at 1065 nm," *Opt. Lett.*, **35** [7] 922–4 (2010).

¹⁰X. D. Xu, Z. W. Zhao, P. X. Song, G. Q. Zhou, J. Xu, and P. Z. Deng, "Structural, Thermal, and Luminescent Properties of Yb-Doped $\text{Y}_3\text{Al}_5\text{O}_{12}$ Crystals," *J. Opt. Soc. Am. B*, **21** [3] 543–7 (2004).

¹¹F. Tang, Y. G. Cao, W. Guo, Y. J. Chen, J. Q. Huang, Z. H. Deng, Z. G. Liu, and Z. Huang, "Fabrication and Laser Behavior of the Yb:YAG Ceramic Microchips," *Opt. Mater.*, **33** [8] 1278–82 (2011).

¹²J. Dong, M. Bass, Y. L. Mao, P. Z. Deng, and F. X. Gan, "Dependence of the Yb^{3+} Emission Cross Section and Lifetime on Temperature and Concentration in Yttrium Aluminum Garnet," *J. Opt. Soc. Am. B*, **20** [9] 1975–9 (2003). □